Ultrasonic/sonic drilling/coring (USDC) for in-situ planetary applications

Yoseph Bar-Cohen[a], Stewart Sherrit[a], Benjamin Dolgin[a], Dharmendra Pal[b], Thomas Peterson[b] Jason Kroh[b], and Ron Krahe[b]

[a] JPL/Caltech, (MS 82-105), 4800 Oak Grove Drive, Pasadena, CA 91109-8099[1]
[b] Cybersonics, Inc., Erie, Pennsylvania

ABSTRACT

A novel ultrasonic drilling and coring device (USDC) was demonstrated to drill a wide variety of rocks: from ice and chalk to granite and basalt. The USDC addresses the key shortcomings of the conventional drills. The device requires low preload (<10 N) and power (down to an average of 5W). The drill bits are not sharpened and, therefore there is no concern to loss of performance due to warring out. The device is not subject to drill walk during core initiation, and, does not apply larger lateral forces on its platform. The USDC has produced round and square cores and 14-cm deep holes and has opened new possibilities to the designers of future NASA planetary exploration missions. USDC can be mounted on a Sojourner class rover, a robotic arm or an Aerobot. USDC itself can perform in very diverse environments and it is an ideal tool for down-the-well delivery of *in-situ* instruments. Since the drill bit does not rotate, many interface problems are simplified. The ultrasonic vibration was observed to transport the drilling debris out of the well. The USDC itself can be used as a sensor for screening drilled objects and the ultrasonic waves produced by the USDC can be used for *in-situ* characterization of rock properties and as a source for sonar. This article describes preliminary modeling of the USDC actuator that predicted various resonance frequencies of the device with a relatively good accuracy. Efforts to develop a comprehensive model that accounts for the properties of the drilled objects are underway. This model should allow optimization of the USDC performance.

Keywords: piezoelectric, drilling, ultrasonic, sonic, USDC, stack, horn, strain amplification, light rovers, planetary exploration.

1. INTRODUCTION

A novel ultrasonic/sonic drilling/coring (USDC) device (see Figure 1) opens new possibilities for future sample return missions. Unlike conventional drilling rigs, USDC can core even the hardest rocks from a very light and flexible platform (e.g., Sojourner, Marie Curie, Aerobot, etc.). The device can be duty cycled without significant loss of efficiency, thus facilitating operations under very low power. Unlike conventional drills, the drilling head of the USDC does not have any gears or motors, it has only two moving parts, and, thus, can be easily adapted to operations in a very wide temperature ranges. The drilling tool does not require sharpening, its drilling speed does not decline with time, and it does not rotate. USDC can core arbitrary cross-sections (square, round, hexagons). Since conventional rotary drills and corers cannot meet these capabilities of USDC, novel mission designs and drilling platforms (e.g., robotic arms, Aerobots) become possible.

Conventional rotary corers limit the possible sample return mission designs. Typically, a rotary corer that produces 10-mm cores in hard rocks requires at least 20-30 watts of power. The rigs cannot be duty cycled without staggering loss of efficiency. The drilling motors can demand as much as 3-4 times larger electrical currents than those during continuous operations (vs. less than 20% for USDC). These corers require over 100N of axial preload, 150N being a typical number.

[1] E-mail: yosi@jpl.nasa.gov; website: http://ndeaa.jpl.nasa.gov

During core initiation, the drill walk can induce torques on the drilling platform that may exceed 30N·m and tangential forces in excess of 100N. Drill chatter delivers low frequency (2-10Hz) high force perturbation on the drilling platform. These properties limit conventional corer applications to very stable and massive platforms with very solid anchoring. In hard rocks, conventional drillers and corers lose the advantage that they sometimes demonstrate in soft materials. In hard rocks, conventional corers stop drilling by shearing and spoliation and become grinders. The latter process is accompanied by at least a 300% increase in energy consumed per unit length of the core. In addition, since the grinding mechanism is determined by the compression failure of the rock, the teeth of the corers must be re-sharpened frequently. The sharpness of bits has to be monitored frequently; otherwise, the heat generation at the tip may increase by a factor of 10 with the similar drop in drilling efficiency. Many a drill bit has been burned or melted under these conditions.

Non-traditional (or modern in the oil industry lingo) drilling technologies (laser, electron beam, microwave, jet, etc.) usually are competitive only in applications that are not power limited. Typically, down-the-well energy required to remove a unit volume of rock for modern technologies are the same as grinding and melting, that is 3 and 5 times higher, correspondingly, than that for shear drilling. Unfortunately, the ratio of down-the-well power delivered vs. input power generator is below several per-cent vs. 10%-30% for conventional drills. Thus, many space missions do not have enough power to employ so called "modern" drilling technologies.

The USDC is ideal for the down the well delivery of in-situ instruments. Since the coring bit does not rotate, the interface between the in-situ instrument and the on-board computer is simplified. Novel sensor techniques can take advantage of the ultrasonic waves produces by the USDC. The changes in the resonant properties of the USDC piezoelectric stack are sufficient for the determination of the rock mechanical properties. In addition, the USDC can be used as a source for sonar. Additional sensors can take advantage of the ultrasonic transport the drilling debris out of the well. This paper describes experiments performed to characterize the USDC, as well as preliminary analytical models of the drilling process.

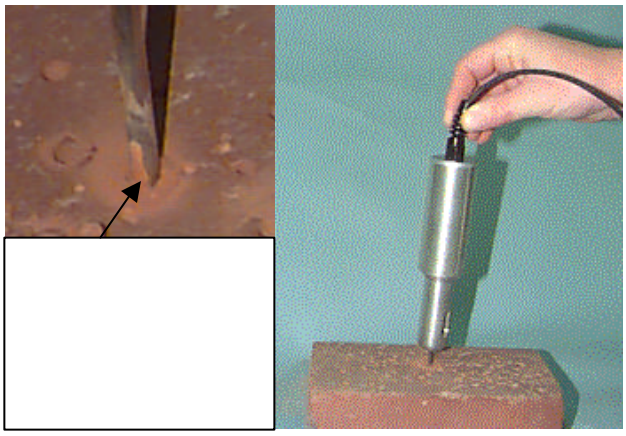

FIGURE 1: Recently developed drilling/coring mechanism (so called USDC) is shown. A relatively small preload is required to create a core. The USDC is shown during drilling while the drilling head is held by its power cord.

2. ULTRASONIC/SONIC DRILLING

The Ultrasonic/Sonic Driller/Corer (USDC) is actuated by a piezoelectric stack [Sherrit, et al, TBP] that drives an ultrasonic horn [Sherrit, et al, 1999a] and a novel ultrasonic/sonic transformer. This transformer consists of a free-floating end-effector (driller or corer), which converts the 20 kHz ultrasonic drive frequency to a combination of this high frequency drive signal and a 60-1000 Hz sonic wave. Additional high frequency components have been detected as well. Conventional ultrasonic drilling mechanisms use only the high frequency micro-hammering action, which is typically slower and requires significantly higher power for comparable drill rates. Figure 1, demonstrates that a relatively low axial preload is required for drilling. The USDC is shown being held by its power cord while drilling a brick. Experiments show that the required force does not change with the rock hardness. The non-criticality of alignment and the fact that the drilling debris travels along the core shaft away from the hole can also be seen in Figure 1. As a result of the transverse and longitudinal motions involved with

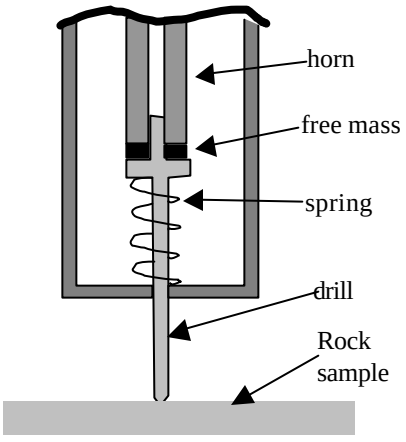

Figure 2 Schematic cross section of the drill assembly with restoring spring and free mass.

this drilling mechanism, the coring bit creates a hole that is slightly larger than the drill bit diameter. This reduces the chances of bit jamming if the integrity of the hole is maintained, thus avoiding one of the problems associated with conventional drilling. The ultrasonic bit does not have to be sharp, or round, and drill bits of various shapes have been used to demonstrate this novel capability. A schematic of the drill is shown in Figure 2.

3. MODELING OF THE USDC ACTUATION

The key elements of the USDC are the piezoelectric stack and the ultrasonic horn, which reside in the actuator assembly. The stack is held in compression by a stress bolt and backed by two layers, b1 and b2, as shown schematically in Figure 3. Using Mason's model an equivalent circuit was drawn (see Figure 4) showing the mechanism of operation of the USDC operation as an electric circuit.

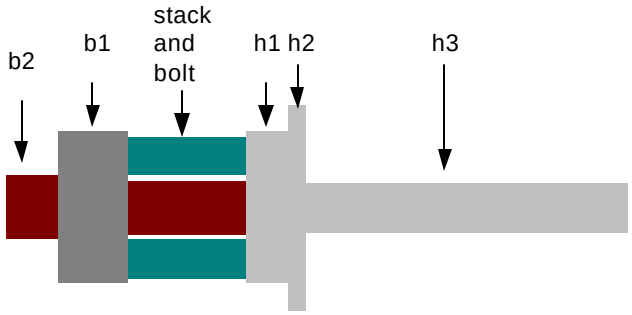

FIGURE 3: Schematic description of the USDC components: horn, stack with stress bolt and backing layers,

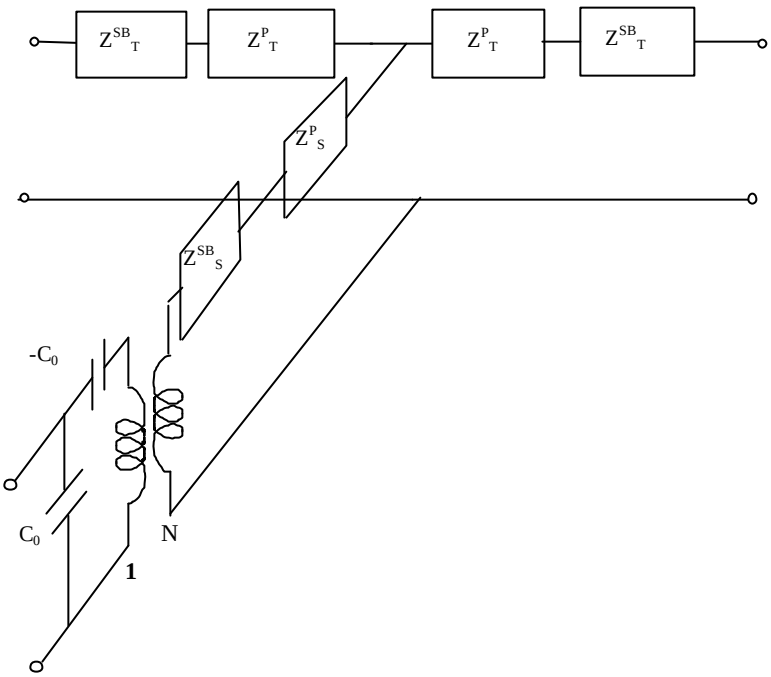

FIGURE 4: Equivalent circuit of the actuator stack and the stress bolt (based on Mason's Model).

3.1 Piezoelectric Stack and Stress Bolt

The piezoelectric stack and stress bolt are modeled using Mason's equivalent circuit for a length extensional resonator (see Figure 4). In order to obtain this model, we use the network representation of a non-piezoelectric solid acoustic element as described by [Redwood, 1961 and McSkimmin, 1994]. For this model we assume that the stress bolt has mechanical impedance that is about 1/6 of the piezoelectric stack and that the strain in the piezoelectric stack and the stress bolt are constant. This means that the acoustic elements in Mason's equivalent circuit should be added in a series to the piezoelectric stack and the stress bolt. The area of the stack is $A=\pi(r_2^2 - r_1^2)$ and the total length of the stack and stress bolt is $L = nt$, where n is the number of layers in the stack and t is the thickness of the layer. The parameters of the Mason's equivalent circuit for the ring stack and stress bolt (see Figure 2) are described in the following equations

$$C_0 = \frac{n^2 \varepsilon_{33}^T A}{L}(1 - k_{33}^2) \tag{1}$$

$$N = \frac{nA}{L}\frac{d_{33}}{s_{33}^E} \tag{2}$$

$$Z_S^{SB} = \frac{Z_0^{SB}}{i \sin(\Gamma^{SB} L)} \tag{3}$$

$$Z_S^P = \frac{Z_0^P}{i \sin(\Gamma^P L)} \tag{4}$$

$$Z_T^{SB} = iZ_0^{SB} \tan(\Gamma^{SB} \frac{L}{2}) \tag{5}$$

$$Z_T^P = iZ_0^P \tan(\Gamma^P \frac{L}{2}) \tag{6}$$

where $Z_0 = \rho v A$ is the specific acoustic impedance which is the product of the density, velocity and area of the acoustic element. The superscripts designate whether the value corresponds to the stress bolt SB or the piezoelectric P. $\Gamma = \omega/v$ is the complex propagation constant for each material where v is the velocity of the acoustic element. The velocity of the piezoelectric is $v = (1/\rho s^D_{33})^{1/2}$ where s^D_{33} is the complex open circuit compliance in the poling direction. The wave velocity for the stress bolt is

$$v = \left(\frac{Y}{\rho}\right)^{1/2} \tag{7}$$

where Y = Y(1+i/Q) is the complex Young's modulus. Q is the mechanical Q of the material.

3.2 Backing layers

The backing layer can be represented by two acoustic elements with matched boundary conditions (see Figure 5). The elements of the acoustic network of the backing layer are

$$Z_T^{B1} = iZ_0^{B1} \tan(\Gamma^{B1} \frac{b_1}{2}) \tag{8}$$

$$Z_S^{B1} = \frac{Z_0^{B1}}{i \sin(\Gamma^{B1} b_1)} \tag{9}$$

$$Z_T^{B2} = iZ_0^{B2} \tan(\Gamma^{B2} \frac{b_2}{2}) \tag{10}$$

$$Z_S^{B2} = \frac{Z_0^{B2}}{i \sin(\Gamma^{B2} b_2)} \tag{11}$$

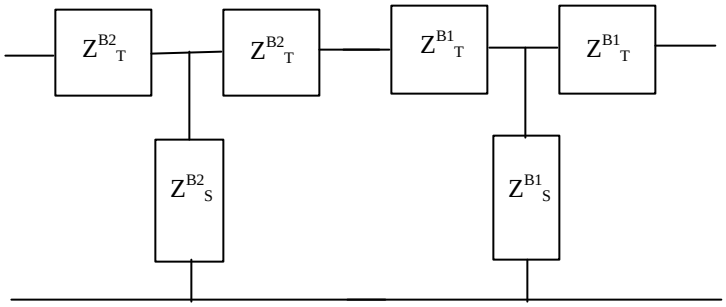

FIGURE 5: Equivalent circuit of the backing layers based on network representation of an acoustic element.

where b_i , Z^i_0, Γ^i are the length, specific acoustic impedance and complex propagation constant of the i^{th} layer. The total acoustic impedance of the backing stack and stress bolt up to the center of the acoustic transmission line is

$$Z_L = Z_T^{SB} + Z_T^P + Z_T^{B1} + \left(\frac{Z_S^{B1}\left(Z_T^{B1} + Z_T^{B2} + \frac{Z_T^{B2} Z_S^{B2}}{Z_S^{B2} + Z_T^{B2}} \right)}{Z_S^{B1} + Z_T^{B1} + Z_T^{B2} + \frac{Z_T^{B2} Z_S^{B2}}{Z_S^{B2} + Z_T^{B2}}} \right) \tag{12}$$

3.3 Horn

The horn equivalent circuit is similar to the model for the backing layer except for an additional layer that is present. It is interesting to note that the stepped horn response discussed by [Belford, 1960] is inherent in the response of two or more network representations of acoustic element. For the acoustic layers (see Figure 4), each layer in the horn is a T network of the tan and sin functions, however due to space limitations we show the T network as a single three port element.

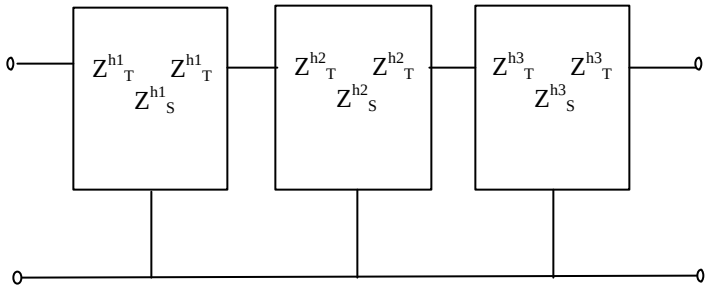

FIGURE 6. The equivalent circuit of the horn based on the network representation of an acoustic element. Each layer is a T network element.

The acoustic impedance of the right side of the acoustic transmission line, which includes the unloaded and unclamped horn, is found by shorting the right side of the network and calculating the effective impedance looking down the left terminals. The impedance is

$$Z_R = Z_T^{SB} + Z_T^P + Z_T^{h1} + \left(\frac{Z_S^{h1}\left(Z_T^{h1} + Z_T^{h2} + \frac{Z_S^{h2}\left(Z_T^{h2} + Z_T^{h3} + \frac{Z_T^{h3} Z_S^{h3}}{Z_T^{h3} + Z_S^{h3}} \right)}{Z_S^{h2} + \left(Z_T^{h2} + Z_T^{h3} + \frac{Z_T^{h3} Z_S^{h3}}{Z_T^{h3} + Z_S^{h3}} \right)} \right)}{Z_S^{h1} + Z_T^{h1} + Z_T^{h2} + \frac{Z_S^{h2}\left(Z_T^{h2} + Z_T^{h3} + \frac{Z_T^{h3} Z_S^{h3}}{Z_T^{h3} + Z_S^{h3}} \right)}{Z_S^{h2} + \left(Z_T^{h2} + Z_T^{h3} + \frac{Z_T^{h3} Z_S^{h3}}{Z_T^{h3} + Z_S^{h3}} \right)}} \right) \tag{13}$$

For a given harmonic force on the front face of the horn the velocity v and the displacement d = v/iω of the tip of the horn can be determined by finding the current through the acoustic impedance Z_T^{h3} at the end of the horn. The total acoustic impedance for the case where the front and back acoustic ports are shorted (free to expand)

$$Z_A = Z_S^{SB} + Z_S^P + \frac{Z_R Z_L}{Z_R + Z_L} \tag{14}$$

where Z_L and Z_R are the sum of the acoustic impedances on the left and right side of the piezoelectric material as defined in (12) and (13). The total electrical impedance as seen from the electrical port is

$$Z = \frac{Z_C\left(\frac{Z_A}{N^2} - Z_C\right)}{\frac{Z_A}{N^2}} = Z_C - \frac{Z_C^2 N^2}{Z_A} \tag{15}$$

where $Z_C = 1/i\omega C_0$. And N is the turns ratio defined in (2). The properties of the elements of the horn are shown in Table 1. We have used the unclamped velocity in the model since at these frequencies the elements are not laterally clamped. That is $v = (Y/\rho)^{1/2}$ where Y is the Young's modulus and ρ is the density.

The impedance of the horn was measured as a function of frequency using a Solatron 1260 Impedance Analyzer. The data and the predicted impedance data are shown in Figure 7. The predicted impedance data was generated using equation 15 and the properties in Table 1. As can be seen, the fit is very good around the first two resonance frequencies. The peak in the impedance spectra at 45 kHz was found to be due to the ring-breathing mode of the piezoelectric stack. The first resonance peak at about 20 kHz is the resonance of the horn tip. The resonance at 35 kHz is associated with resonance of the full assembly (horn, backing and stack). The slight mismatch in the reactance data at the resonance of the horn (35 kHz) tip is due to the large Q of the resonators. If the data is measured on a finer frequency scale a better visual match to the data is observed.

Table 1. Properties of the horn elements used in the modeling

Piezoelectric Stack
ID. = 0.0125 m OD.=0.025 m L= 0.0212 m
ρ =7800 kg/m^3 n=4
d_{33} = 280(1-0.0008i) pC/N
ε^T_{33} = 1.09x10^{-8}(1-0.0015i) F/m
s^E_{33} = 2.0x10^{-11}(1-0.0012i) m^2/N
Stress Bolt
OD.=0.00952 m L= 0.0212 m ρ =7890 kg/m^3
v = 4970(1+0.001i) m/s
Backing Layer 1
OD.=0.0268 m L= 0.0127 m ρ =7890 kg/m^3
v = 4970(1+0.001i) m/s
Backing Layer 2
OD.=0.011 m L= 0.00902 m ρ =7890 kg/m^3
)70(1+0.001i) m/s
Horn Layer 1
OD.=0.0268 m L= 0.00775 m ρ =4430 kg/m^3
v = 5150(1+0.0006i) m/s
Horn Layer 2
OD.=0.0366 m L= 0.00325 m ρ =4430 kg/m^3
v = 5150(1+0.0006i) m/s
Horn Layer 3
OD.=0.00890 m L= 0.0583 m ρ =4430 kg/m^3
v = 5150(1+0.0006i) m/s

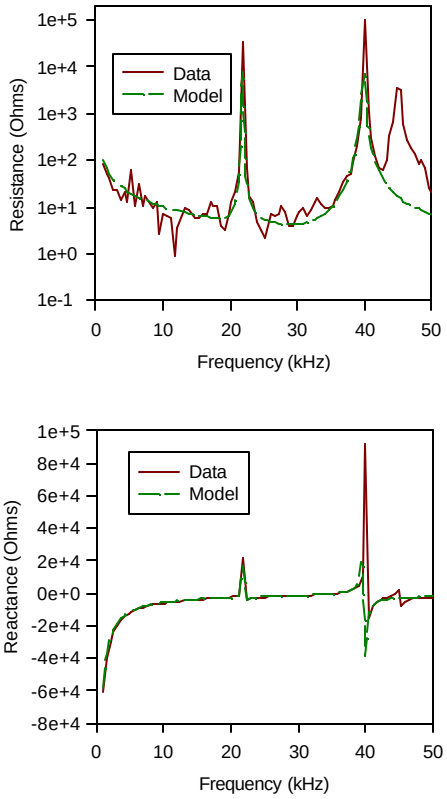

FIGURE 7: The impedance resonance of the piezoelectric stack, horn and backing. The data and the fit to the data based on the model presented in the text with the constants shown in Table 1.

4. EFFECT OF LOAD

In our current drill design an ultrasonic horn driven at 20-23 kHz is used to excite a free-floating drill or coring bit into various rock samples. The action is similar to a jackhammer impact. Although the electrical drive is of the order of 20 kHz, considerable low frequency components are present in the drill. The load on the horn tip is non-linear and substantial sub-

harmonics are produced which aid in the drilling process. The drill is in contact with the horn tip and is driven from the horn at the horn tip velocity. The tip of the drill or corer is impacted into the rock sample creating stress fracture in the material. An optional restoring spring is used to aid in returning the drill base to the horn tip where the action is repeated. A free mass between the horn and drill bass was found to increase the low frequency energy transfer as well as reduce the dependence of the drilling rates on the drill stem length.

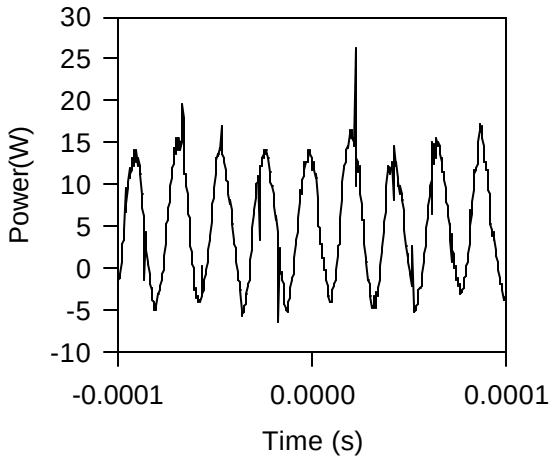

FIGURE 8. The power to the horn during drilling into construction brick with a tungsten carbide steel rod (2.75 mm diam) and a 4-g free mass. The average consumed power was 5.3-watts. The drill rate was 0.1-mm/s.

The power dissipated in the drill while drilling into construction brick is shown in Figure 8, where the average power dissipated in this case is 5.3 watts. Measurements of the accoustic power spectrum in the rock samples as well as audible noise during drilling indicates a substantial low frequency component in the drill bit. Current efforts are underway to model the source of these low frequency components. At present it is believed that the free mass, drill base, drill stem and rock sample structure is driven by resonance of the horn. Because the horn tip and the free mass are weekly coupled, the drill assembly experiences a large impulse force when in contact with the horn. Since the contact is random due to the time of flight of the drill stem and the amount of energy deposited into the rock a distribution in low frequency pulses results. As well a constant small normal force is required to feed the drill into the rocks.

5. APPLICATIONS OF USDC

The unique capabilities that were observed when operating the USDC has enabled new technologies and opportunities both planetary and terrestial, where low axial load is used with no need for torque. For space applications in-situ sampling is being explored, where as for earth applications we are considering commerical, geological, medical, military and other applications. To determine the scope of the USDC capability we drilled and cored such rocks as diorite, magnetite, sandstone, limstone, and basalt as well as ice, silicon and construction brick. To demonstrate the viability of the USDC it was mounted on the Mars Pathfiner's Sojourner class rover using a plastic tube holder and it was demonstrated to drill through 14-cm thick sandstone (see Figure 9). This success led to a recent initiative to develop a USDC for consideration of launched in a Mars mission as early as the year 2003.

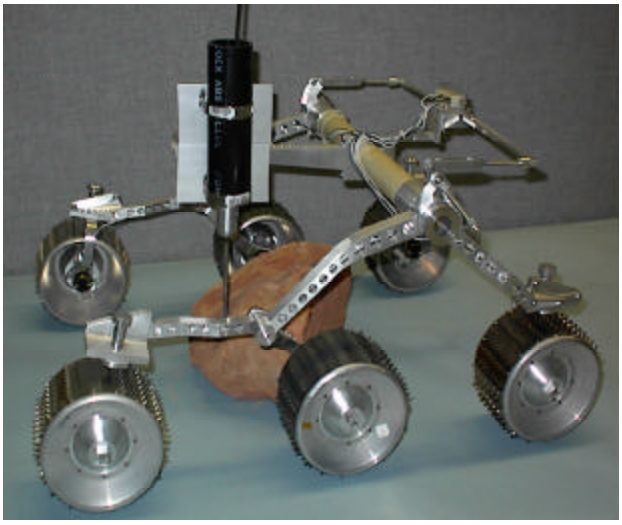

FIGURE 9: Drilling rocks using a USDC that is mounted on a Sojourner class rover.

6. CONCLUSIONS

Recently, a novel ultrasonic/sonic driller/corer (USDC) mechanism was developed that requires relatively low power and low axial load and drill rocks have hardness that range from very hard (e.g., basalt and granite) to very soft (e.g., chalk, sand stone, etc.). Preliminary efforts were made to model the actuator of the USDC and the various resonance frequencies were predicted with a relatively good accuracy. Efforts are currently underway to develop a comprehensive model that accounts for the drilled objects to allow optimization of the drilling performance. In parallel, initiatives are being taken in a variety of areas including space to terrestrial to develop and demonstrate applications that can improve and simplify the process of drilling and coring. USDC is currently being sought for use to allow bringing samples from other planets using low power and operating from very lightweight platforms (balloon, rover, lander, etc.).

ACKNOWLEDGMENT

The research at Jet Propulsion Laboratory (JPL), California Institute of Technology, was carried out under a contract with National Aeronautics and Space Agency (NASA) Code S, as part of the Surface Systems Thrust area of CETDP, Program Manager Dr. Samad Hayati and Task Manager, Dr. Chester Chu. The development at Cybersonics was conducted under a JPL/NASA SBIR Phase II contract, whose Technical Manager is this paper principal author.

REFERENCES

Bar-Cohen Y., S. Sherrit, B. Dolgin, T. Peterson, D. Pal and J. Kroh, "Ultrasonic/Sonic Driller/ Corer (USDC) With Integrated Sensors," New Technology Report, Docket No. 20856, Item No. 0448b, November 17, 1999.

Belford, J.F., "The Stepped Horn", Proceedings of the National Electronics Conference, Chicago, IL, (1960), pp. 814-822.

McSkimmin H.J., Ultrasonic Methods for Measuring the Mechanical Properties of Liquids and Solids, Volume 1-Part A, ed. W.P. Mason Academic Press, New York, 1964

Redwood M., "Transient Performance of a Piezoelectric Journal of the Acoustical Society of America, **33**, pp.527-536, 1961

Sherrit S., B. P. Dolgin, Y. Bar-Cohen, D. Pal, J. Kroh, and T. Peterson, "Modeling of Horns for Sonic/Ultrasonic Applications," Proceedings of the IEEE International Ultrasonics Symposium, held in Lake Tahoe, CA, 17-20 October 1999a.

Sherrit S., S. P. Leary, and Y. Bar-Cohen "Comparison of the Mason and KLM Equivalent Circuits for Piezoelectric Resonators in the Thickness Mode," Proceedings of the IEEE International Ultrasonics Symposium, held in Lake Tahoe, CA, 17-20 October 1999b.

Sherrit S., S. P. Leary, B. P. Dolgin, Y. Bar-Cohen and R. D. Tasker, "The Impedance Resonance for Piezoelectric Stacks," To be submitted to J. of Acoustic Society of America.